University of Pennsylvania
ScholarlyCommons

Departmental Papers (CBE)

Department of Chemical & Biomolecular Engineering

January 2007

A Strategy for Achieving High-performance with SOFC Ceramic Anodes

Michael D. Gross
University of Pennsylvania

John M. Vohs
University of Pennsylvania, vohs@seas.upenn.edu

Raymond J. Gorte
University of Pennsylvania, gorte@seas.upenn.edu

Follow this and additional works at: http://repository.upenn.edu/cbe_papers

Recommended Citation
Gross, M. D., Vohs, J. M., & Gorte, R. J. (2007). A Strategy for Achieving High-performance with SOFC Ceramic Anodes. Retrieved from http://repository.upenn.edu/cbe_papers/86

Postprint version. Copyright The Electrochemical Society, Inc. 2007. All rights reserved. Except as provided under U.S. copyright law, this work may not be reproduced, resold, distributed, or modified without the express permission of The Electrochemical Society (ECS). The archival version of this work was published in *Electrochemical and Solid-State Letters*, Volume 10, Issue 4, 2007, pages B65–B69.
Publisher URL: http://scitation.aip.org/ESL/

This paper is posted at ScholarlyCommons. http://repository.upenn.edu/cbe_papers/86
For more information, please contact repository@pobox.upenn.edu.

A Strategy for Achieving High-performance with SOFC Ceramic Anodes

Abstract
A proposal that high solid oxide fuel cell (SOFC) anode performance can be achieved by using a very thin, catalytically active functional layer, with a noncatalytic conduction layer, has been tested. An anode impedance of 0.26 Ω cm^2 was obtained at 973 K in humidified H_2 using a Ag-paste conduction layer and a 12 μm thick functional layer made from 1 wt % Pd and 40 wt % ceria in yttria-stabilized zirconia. Replacing the Ag paste with a 100 μm layer of porous $La_{0.3}Sr_{0.7}TiO_3$ (LST) had minimal effect on cell performance. The anode concept is flexible and should allow various materials to be used in the functional and the current-collector layers.

Comments
Postprint version. Copyright The Electrochemical Society, Inc. 2007. All rights reserved. Except as provided under U.S. copyright law, this work may not be reproduced, resold, distributed, or modified without the express permission of The Electrochemical Society (ECS). The archival version of this work was published in *Electrochemical and Solid-State Letters*, Volume 10, Issue 4, 2007, pages B65–B69.
Publisher URL: http://scitation.aip.org/ESL/

This journal article is available at ScholarlyCommons: http://repository.upenn.edu/cbe_papers/86

A strategy for achieving high-performance with SOFC ceramic anodes

M. D. Gross, J. M. Vohs, and R. J. Gorte
Department of Chemical & Biomolecular Engineering
University of Pennsylvania
Philadelphia, PA 19104

Abstract

A proposal that high SOFC anode performance can be achieved by using a very thin, catalytically active functional layer, with a non-catalytic conduction layer, has been tested. An anode impedance of 0.26 $\Omega \cdot cm^2$ was obtained at 700°C in humidified H_2 using a Ag-paste conduction layer and a 12-µm thick functional layer made from 1-wt% Pd and 40-wt% ceria in YSZ. Replacing the Ag paste with a 100-µm layer of porous $La_{0.3}Sr_{0.7}TiO_3$ (LST) had minimal effect on cell performance. The anode concept is flexible and should allow various materials to be used in the functional and the current-collector layers.

Introduction

Most developers of solid oxide fuel cells (SOFC) are using anodes that are a mixture of Ni and an ion-conducting ceramic material, such as yttria-stabilized zirconia (YSZ) [1,2]. These ceramic-metallic (cermet) composites are capable of outstanding performance in H_2 or syngas (a mixture of CO and H_2 formed by hydrocarbon reforming); however, the Ni-cermet anodes also suffer from limitations, the lifting of which could speed the commercialization of this technology. Ni cermets are sensitive to the presence of sulfur in the fuel [3], they cannot tolerate being oxidized during start-up and shut-down cycles [4], and they can be severely damaged by carbon formation if exposed to dry hydrocarbons [5].

As replacements for Ni-cermet anodes, two different types of materials have been proposed, each with its own advantages and disadvantages. First, based largely on work at Penn, Cu-ceria cermets were suggested, with the primary goal that these materials can be used for direct utilization of hydrocarbons [5,6]. Cu does not catalyze the formation of carbon fibers the way that Ni does but is also not a good oxidation catalyst. In the Cu-based anodes, Cu is believed to provide only electronic conductivity, while ceria is the mixed conductor/oxidation catalyst responsible for electrochemical oxidation of the hydrocarbon. Cu-ceria composites have demonstrated reasonable performance using liquid fuels [7], and have exhibited excellent sulfur tolerance [8]. However, Cu-based anodes cannot tolerate oxidation cycles and show poor thermal stability above 700ºC [9]. The reason for the poor thermal stability is that Cu has a relatively low melting temperature and a low surface energy, causing it to sinter easily at high temperatures. Sintering, in turn, leads to a loss in anode conductivity [10].

The other class of materials that has been investigated extensively for replacing Ni cermets is conductive ceramics [11-17]. Like Cu, ceramic anodes are stable against carbon-fiber formation in hydrocarbon fuels; and, depending on the particular ceramic that is used, ceramic anodes can be sulfur tolerant [17]. Ceramic anodes have the additional desirable properties that they can be insensitive to oxidation and reduction cycles and they can exhibit excellent thermal stability. Unfortunately, the performance of most ceramic anodes has been modest compared to that achieved by cells with Ni cermets. Typically, SOFC with ceramic anodes must be operated at higher temperatures to produce comparable power densities and anode overpotentials. For example, most studies with ceramic anodes are carried out at temperatures above 900°C, whereas good power densities (>500 mW/cm^2) are routinely achieved on SOFC with Ni-YSZ cermets at

temperatures below 700ºC [18]. One exception to this rule is the recent report by Huang, et al [15,16], who achieved very high performance using a complex, double perovskite. While those results appear very promising, the stability of this material against interfacial reactions with YSZ, the usual electrolyte of choice [11], is uncertain.

The material requirements for achieving high performance with ceramic anodes have been outlined in a review by Atkinson, et al [2]. These authors have argued that alternative anode materials must have a conductivity of at least 1 S/cm at $P(O_2)$ of approximately 10^{-20} atm. (An electrode that is 1 mm thick and has a conductivity of 1 S/cm would have a resistance of 0.1 $\Omega \cdot cm^2$, an upper limit for the maximum losses which can be tolerated.) Because the electrode must be porous to allow fuel to diffuse to the three-phase boundary, the materials making up the anode must have intrinsic conductivities somewhat higher than 1 S/cm. While there are a number of oxides that meet the minimum conductivity requirements, it is more difficult to identify conductive oxides that also exhibit ionic conductivity, surface reactivity with O_2, chemical compatibility with YSZ, and compatible thermal expansion with YSZ. Much of the effort to identify appropriate materials has focused on perovskites with a mixture of cations at the B sites, with the objective of obtaining complimentary functionality from appropriate cation combinations without seriously degrading the good properties induced by the individual ions [11].

In this paper, we propose an approach analogous to what has been utilized extensively with Ni-cermet anodes, in which the electrode is separated into two distinct layers, a thin functional layer near the electrolyte to perform the electrochemical reaction and a separate conducting layer for current collection [18,19]. However, while the materials used in both the functional and conduction layers are usually similar with Ni cermets, we propose using different materials for each layer, with the materials in the functional layer optimized for catalytic activity and the materials in the conduction layer optimized for conductivity. If the functional layer is thin enough, its conductivity can be low. For example, the criterion that electrode losses should be less than 0.1 $\Omega \cdot cm^2$ only requires the material in the functional layer to have a conductivity of 0.01 S/cm if the thickness of the functional layer is 10 μm thick.

In the present paper, we will demonstrate that excellent performance can indeed be achieved using an anode having a functional layer made from Pd-doped ceria in YSZ and a conduction layer made from LST ($La_{0.3}Sr_{0.7}TiO_3$). Because the concept is flexible, we suggest

that high performance can be achieved with other materials providing the catalytic activity and conductivity.

Experimental

The general approach for cell fabrication involved synthesis of the electrodes by impregnation of porous YSZ and has been described previously [20,21]. First, a YSZ wafer was prepared with two porous layers separated by a dense layer. In this study, the dense layer was 75-µm thick and the two porous layers were 300-µm and either 12 or 50-µm thick. The YSZ wafers were prepared by laminating together three green tapes, with pore formers included in the tapes for those layers requiring porosity. Porosity in the 300-µm layer was obtained using a mixture of graphite and polystyrene pore formers, while the thinner porous layer used only graphite. The tapes were fired to 1823 K for 4 h to produce the YSZ wafer, with porosities of approximately 65% on both sides of the electrolyte. For cells using LST as the current-collection layer of the anode, a glycerol slurry of LST powder was pasted onto the 12-µm, porous YSZ and the cell was then fired again to 1823 K to provide a structure like that shown in Fig. 1.

The LSF-YSZ composite cathodes were fabricated by impregnation of the 300-µm porous YSZ with aqueous solutions containing $La(NO_3)_3 \cdot 6H_2O$, $Sr(NO_3)_2$, and $Fe(NO_3)_3 \cdot 9H_2O$ at a molar ratio of La:Sr:Fe = 0.8:0.2:1, followed by calcination to 1123 K [22]. Multiple impregnation steps were used to reach a final loading of 40-wt% LSF. The porous YSZ in the anode layer was then impregnated with CeO_2 and Pd using the corresponding nitrate salts. Finally, Ag paste and Ag wire were applied to both the anode and cathode sides for current collection.

For fuel-cell testing, the cells were attached to an alumina tube with a ceramic adhesive (Aremco, Ceramabond 552). Impedance spectra were measured at 0.2 A/cm^2 in the galvanostatic mode with a frequency range of 0.1 Hz to 100 KHz and a 1-mA AC perturbation using a Gamry Instruments potentiostat. The active area of the cells, equal to the anode area, was 0.33 cm^2; but the area of the electrolyte and cathode were approximately 1 cm^2. H_2 and CH_4 were introduced to the anode compartment through a room-temperature, water bubbler for humidification. The fuel flow rates were 50 ml/min for both fuels, resulting in fuel utilizations of less than 7% for H_2 and less than 1% for CH_4.

Results

The initial experiments simply used Ag as the current collector. The results in Fig. 1 were achieved in humidified (3% H_2O) H_2 using a cell with a functional layer made from the 12-μm thick, porous YSZ, impregnated with 40-wt% CeO_2 and 1-wt% Pd. A composite of Pd, ceria, and YSZ was chosen for this study because Pd/ceria is one of the most active hydrocarbon-oxidation catalysts [23]. Furthermore, ceria has some electronic conductivity under reducing conditions and composites formed by impregnation into porous YSZ have a coefficient of thermal expansion (CTE) similar to YSZ because YSZ forms the backbone of the structure [24].

Fig. 1a) shows that the V-i polarization curves were linear at the lower current densities and that reasonable power densities, 249 mW/cm^2 at 923 K and 865 mW/cm^2 at 1073 K, could be reached at intermediate temperatures, even using a relatively thick YSZ electrolyte. Information on factors that limit cell performance can be obtained from the Cole-Cole Plots of the impedance spectra in Fig. 1b). The ohmic resistances of the cell are determined from the high-frequency intercepts with the abscissa in the Cole-Cole plots, while the total cell resistances, which are equal to the slopes of the V-i curves, are equal to the low-frequency intercepts with the abscissa. The results indicate that the cell losses are dominated by ohmic losses, which arise primarily from the 75-μm thick electrolyte. Using literature values for the conductivity of YSZ ($\sigma = T^{-1} \times 3.6\times10^5$ S·K/cm x exp{-8x10^4 J/mol/RT}) [25], the contributions to the ohmic resistance from the electrolyte ranged from 0.65 Ω·cm^2 at 650°C to 0.175 Ω·cm^2 at 800°C. At all temperatures, the differences between the ohmic losses measured by impedance spectroscopy and the calculated resistances of the electrolyte were less than 0.1 Ω·cm^2.

Obviously, the non-ohmic losses for the cell in Fig. 1 contain contributions from both the anode and cathode. We did not attempt to separate anode and cathode losses using reference electrodes because of the intrinsic errors that are present in these measurements when using thin electrolytes [26-28]; however, cathode losses for LSF-YSZ composites of type used in this study have been determined to be approximately 0.1 Ω·cm^2 at 700°C [22]. This would suggest that the anodic losses for the cell in Fig. 1 were approximately 0.26 Ω·cm^2 at 700°C, using the calculated electrolyte loss of 0.40 Ω·cm^2 for this temperature.

The addition of dopant levels of a catalytic metal, Pd in this case, is crucial for achieving high catalytic activity and the high performance. The results in Fig. 2, which are also tabulated in Table 1, were obtained on a cell identical to that used for the data in Fig. 1, except that no Pd was added. At each temperature studied, the maximum power densities were lower by a factor of

approximately four. The ohmic resistances were also slightly larger (e.g. At 973 K, the ohmic resistance was 0.55 $\Omega \cdot cm^2$, compared to 0.49 $\Omega \cdot cm^2$ on the cell with Pd.), but most of the decreased performance was associated with the non-ohmic, electrode polarization losses. Because the amount of added Pd was too small to contribute to electrode conductivity in the first cell, we suggest that Pd promotes the reduction of ceria, a property well known from heterogeneous catalysis [29], thereby slightly increasing the conductivity of the functional layer. Finally, the differences in the performance of cells with and without Pd demonstrate that Ag is not providing significant catalytic activity, an expected result given that Ag is not a good oxidation catalyst.

To test the effect of anode functional-layer thickness, we prepared another cell with 1-wt% Pd and 40-wt% ceria, but using a 50-μm (rather than 12-μm) thick, porous YSZ layer. Again, the maximum power densities and ohmic resistances are listed in Table 1. The maximum power densities decreased with the increased thickness of the functional layer and at least some of the lost performance is due to increased ohmic resistances. For example, at 973 K, the ohmic resistance increased from 0.49 $\Omega \cdot cm^2$ to 0.74 $\Omega \cdot cm^2$. Calculating the conductivity of the functional layer from the differences in the ohmic resistances and the functional-layer thickness, we obtain a value of 0.015 S/cm. Notice that the ohmic contribution of a 12-μm thick functional layer would be 0.08 $\Omega \cdot cm^2$, in good agreement with the difference between the ohmic losses (0.49 $\Omega \cdot cm^2$) and the calculated electrolyte losses (0.40 $\Omega \cdot cm^2$) for the cell in Fig. 1. A conductivity of 0.015 S/cm is significantly below that normally targeted for anode materials and also well below that expected for bulk ceria under these conditions [2]. The increase in the non-ohmic impedance with thickness of the functional layer is probably related to the poor conductivity of this layer, given that a similar increase has been reported in the non-ohmic losses following sintering in Cu-based anodes [10].

Obviously, the Ag paste in the cells just described plays a crucial role for conduction and should be considered part of the anode. To determine the effect of using an electronically conductive ceramic in the current-collection layer, we prepared a cell with the same 12-μm functional layer used earlier (1-wt% Pd and 40-wt% ceria in YSZ) and a 100-μm current-collection layer of porous $La_{0.3}Sr_{0.7}TiO_3$ (LST). LST was chosen for this study because it has a similar CTE to that of YSZ and does not react with YSZ, even after co-firing at 1823 K [30,31]. Furthermore, LST has no ionic conductivity and is a poor electrocatalyst, so that there is no

ambiguity about the role that this layer plays. Except for heating the LST layer in humidified H_2 up to the operating temperature of the cell, we performed no special reduction of the LST to improve its conductivity. Performance data for the LST cell in humidified H_2 and humidified CH_4 are shown in Figs. 3 and 4.

In humidified H_2, the power densities achieved with the LST current collector were slightly lower than that with the Ag current collector, but still quite respectable. For example, the maximum power densities at 973 K and 1073 K were 339 and 653 mW/cm^2, respectively. Considering the impedance data for the cells with LST (Fig. 3b) and Ag (Fig. 1b) current collectors, the performance differences are due primarily to a slightly higher ohmic resistance in the cell with the LST current collector. For example, at 973 K, the LST cell had an ohmic resistance of 0.58 $\Omega \cdot cm^2$, compared to 0.49 $\Omega \cdot cm^2$ on the Ag cell. The non-ohmic impedances for the two cells at 973 K were similar, 0.27 $\Omega \cdot cm^2$ on the LST cell and 0.22 $\Omega \cdot cm^2$ on the Ag cell.

Because one of the goals in using a ceramic anode is to operate in hydrocarbon fuels, we also tested the LST cell in humidified (3% H_2O) CH_4, with the results shown in Fig. 3. Since the fuel utilization in these tests was less than 1%, negligible amounts of water were generated in the anode. The first intriguing aspect of the data is that the open-circuit voltages (OCV) at each temperature were greater than 1.15 V, a value higher than that which would be achieved with humidified H_2 or CO. Therefore, it is unlikely that the high OCV can be explained by considering the electrochemical reaction to be occurring through a reforming process, suggesting that the hydrocarbon is probably oxidized directly. Second, the maximum power densities approach that observed with humidified H_2, with maximum power densities of 208 mW/cm^2 at 973 K and 539 mW/cm^2 at 1073 K. Finally, the anode exhibited no evidence for carbon formation during an overnight exposure to CH_4.

Discussion

As pointed out in the Introduction, it is very difficult to devise oxide-based electrodes that have good electronic and ionic conductivity, high surface reactivity with O_2, and good chemical compatibility with YSZ. What we have demonstrated is that it is possible to decouple the catalytic properties from the conduction properties by using completely different materials in the two layers. While the idea of separating the electrode into functional and conduction layers is certainly not new, it is more unusual to use completely different materials for the two layers. The choice of a material that is optimized primarily for catalytic activity in the functional layer,

without regard for conductivity, is also unusual. Obviously, some conductivity is required in the functional layer; but, as we have shown, the conductivity can be quite low.

Because dopant levels of Pd were added to the high-performance anodes in this study, the anodes are not entirely ceramic. However, the volume percent of metal that was added was low enough that it cannot be important for providing conductivity. Furthermore, the metal content in the electrode is small enough that the electrode should not be damaged by oxidation of the metal, making the electrodes redox stable. While we chose to use Pd in this study because of its high activity and its tolerance against carbon formation in the presence of hydrocarbons, many cheaper metals are known to promote the reduction of ceria and it may prove advantageous to use different catalysts for different applications. For example, when using syngas or H_2 as the fuel, Ni promoters would probably be adequate for enhancing the reduction rate of ceria. Different metal catalysts may also be chosen for applications where sulfur tolerance is required, since ceria itself is quite sulfur tolerant [5].

Although ceria is one of the best total-oxidation catalysts among oxides [32,33], it may be possible to replace it with other oxides. An obvious choice would be ceria-zirconia solutions [34], given that these are more easily reduced than pure ceria and exhibit both electronic and ionic conductivity. Another interesting possibility would be to incorporate the double perovskite, $Sr_2Mg_{1-x}Mn_xMoO_{6-\delta}$, investigated by Huang, et al [15,16], given that this material was reported to exhibit high activity for the electrochemical oxidation of methane. Surprisingly, none of the pure-component oxides that make up the double perovskite exhibit high catalytic activity for oxidation reactions, implying that the high activity may be associated with the mixture. Because the authors of that study used Pt paste as the current collector, it must be confirmed that the presence of Pt did not play a role in the performance that they achieved.

Regarding the current-collection layer, it is significant that the results with the Ag and LST current collectors were so similar. This suggests that essentially any material can be used for the conduction layer so long as it has sufficient electronic conductivity and is compatible mechanically and chemically with the functional layer. Again, the results suggest a high degree of flexibility in the choice of materials for the conduction layer.

Conclusions

To conclude, the most important finding in this study is that one can obtain excellent performance using anodes with a thin functional layer and a separate conduction layer, even if

the conductivity of the functional layer is low. The part of the anode responsible for current collection can be treated separately, allowing materials in each layer to be optimized independently. This strategy of designing each layer in the anode independently allows much greater flexibility in electrode design. While we have identified a set of materials capable of achieving outstanding performance, it seems likely that other materials can be identified with even better catalytic and conduction properties.

Acknowledgements

This work was funded by the U.S. Department of Energy's Hydrogen Fuel Initiative. Some of the experiments were performed by Mr. Reum Scott.

References

1. Minh, N. Q. Ceramic fuel cells. J. Am. Ceram. Soc. 76, 563-588 (1993).
2. A. Atkinson, S Barnett, R. J. Gorte, J.T.S. Irvine, A.J. McEvoy, M.B. Mogensen, S. Singhal, and J. Vohs, Advanced anodes for high-temperature fuel cells. Nature Mater. 3, 17-27 (2004).
3. Matsuzaki, Y., Yasuda, I. The poisoning effect of sulfur-containing impurity gas on a SOFC anode: Part I. Dependence on temperature, time, and impurity concentration. Solid State Ionics 132, 261-269 (2000).
4. Rietveld, G., Nammensma, P., Ouweltjes, J. P., in: Yokokawa, H., Singhal, S. C. (Eds.), Proceedings of the Seventh International Symposium on Solid Oxide Fuel Cells (SOFCVII), The Electrochemical Society Proceedings Series, Pennington, NJ, PV 2001-16, p. 125, (2001).
5. McIntosh, S., Gorte, R. J., Direct hydrocarbon solid oxide fuel cells. Chem. Rev. 104, 4845-4865 (2004).
6. S. Park, J. M. Vohs, and R. J. Gorte, *Nature*, **404**, 265 (2004).
7. H. Kim, S. Park, J. M. Vohs, and R. J. Gorte, Journal of the Electrochemical Society, 148 (2001) A693-A695.
8. Hongpeng He, J. M. Vohs, and R. J. Gorte, Electrochemical and Solid State Letters, 8 (2005) A279-280.
9. M. D. Gross, J. M. Vohs, and R. J. Gorte, Journal of the Electrochemical Society, 153 (2006) A1386-90.

10. S. Jung, C. Lu, H. He, K. Ahn, R. J. Gorte, and J. M. Vohs, Journal of Power Sources, 154 (2006) 42-50.
11. Tao, S. & Irvine, J. T. S. Discovery and characterization of novel oxide anodes for solid oxide fuel cells. The Chemical Record 4, 83-95 (2004).
12. Liu, J., Madsen, B. D., Ji, A., & Barnett, S. A. A fuel-flexible ceramic-based anode for solid oxide fuel cells. J. Electrochem. Solid-State Lett. 5, A122-A124 (2002).
13. Marina, O. A., Canfield, N. L., & Stevenson, J. W. Thermal, electrical, and electrocatalytical properties of lanthanum-doped strontium titanate. Solid State Ionics 149, 21-28 (2002).
14. Sfeir, J., Buffat, P.A., Mockli, P., Xanthopoulos, N., Vasquez, R., Mathieu, H. J., Van herle, J., Thampi K. R. Lanthanum chromite based catalysts for oxidation of methane directly on SOFC anodes. J. Catal. 202, 229-244 (2001).
15. Huang, Y-H., Dass, R. I., Xing, Z-L., & Goodenough, J. B. Double perovskites as anode materials for solid-oxide fuel cells. Science 312, 254-257 (2006).
16. Y.-H. Huang, R. I. Dass, J. C. Denyszyn, and J. B. Goodenough, JECS, 153 (2006) A1266.
17. R. Mukundan, E. L. Brosha, & F. H. Garzon, ESSL, 7, A-5 (2004).
18. Zhao F. & Virkar A.V. Dependence of polarization in anode-supported solid oxide fuel cells on various cell parameters. Journal of Power Sources, 141, 79-95 (2005).
19. V. Vashook, J. Zosel, R. Muller, P. Shuk, L. Vasylechko, H. Ullmann, and U. Guth, Fuel Cells, 6 (2006) 293.
20. Gorte, R. J., Park, S., Vohs, J. M., and Wang, C. H. Anodes for direct oxidation of dry hydrocarbons in a solid-oxide fuel cell. Adv. Mater., 12, 1465-1469 (2000).
21. S. Park, R. J. Gorte, and J. M. Vohs, Journal of the Electrochemical Society, 148 (2001) A443-A447.
22. Huang, Y., Vohs, J. M., Gorte, R. J. Fabrication of Sr-doped $LaFeO_3$ YSZ composite cathodes. J. Electrochem. Soc. 151, A646-A651 (2004).
23. Trovarelli, A., Catalytic properties of ceria and CeO_2-containing materials. Catalysis Reviews-Science and Engineering, 38, 439-520 (1996).

24. Huang, Y., Ahn, K., Vohs, J. M., & Gorte R. J. Characterization of Sr-doped $LaCoO_3$-YSZ composites prepared by impregnation methods. J. Electrochem. Soc. 151, A1592-A1597 (2004).
25. K. Sasaki, J. Maier, SSI, 134 (2000) 303.
26. McIntosh, S., Vohs, J. M., & Gorte, R. J. Impedance spectroscopy for the characterization of Cu-Ceria-YSZ anodes for SOFCs. Journal of the Electrochemical Society, 150, A1305-A1312 (2003).
27. S. B. Adler, B. T. Henderson, M. A. Wilson, D. M. Taylor, R. E. Richards, Solid State Ionics, 134 35-42 (2000).
28. M. Mogensen and P. V. Hendriksen (Electrochemical Society Proceedings, Volume 2003-07, pp 1126-1131
29. H. Cordatos and R. J. Gorte, J. Catal., 159, 112 (1996).
30. Kipyung Ahn, Sukwon Jung, John M. Vohs, Raymond J. Gorte, Ceramics International, in press.
31. He, H. Huang, Y., Vohs, J. M. & Gorte, R. J. Characterization of YSZ-YST Composites for SOFC Anodes. Solid State Ionics, 175, 171-176 (2004).
32. S. Zhao and R. J. Gorte, Appl. Catal. A, 248, 9 (2003).
33. S. Zhao and R. J. Gorte, Appl. Catal. A, 277, 129 (2004).
34. K. Ahn, H. He, J. M. Vohs, and R. J. Gorte, Electrochemical and Solid State Letters, 8 (2005) A414-17.

Figure 1 (a) V-i polarization curves and **(b)** impedance spectra on a 12 μm Ce-Pd-YSZ anode with a Ag current collector in humidified H_2 (3% H_2O). Data are shown for the following temperatures: circles, 923 K; diamonds, 973 K; triangles, 1023 K; and squares, 1073 K.

Figure 2 (a) V-i polarization curves and **(b)** impedance spectra on a 12 μm Ce-Pd-YSZ anode with a LST current collector in humidified H_2 (3% H_2O). Data are shown for the following temperatures: circles, 923 K; diamonds, 973 K; triangles, 1023 K; and squares, 1073 K.

Figure 3 (a) V-i polarization curves and **(b)** impedance spectra on a 12 μm Ce-Pd-YSZ anode with a LST current collector in humidified CH_4 (3% H_2O). Data are shown for the following temperatures: diamonds, 973 K; triangles, 1023 K; and squares, 1073 K.

Figure 4 SEM micrographs of the anode region, prior to the addition of catalysts, of the cells used in this study.

Table 1 Comparison of maximum power densities and ohmic resistances of cells with thin functional layer anodes. *fuels were humidified (3% H_2O)

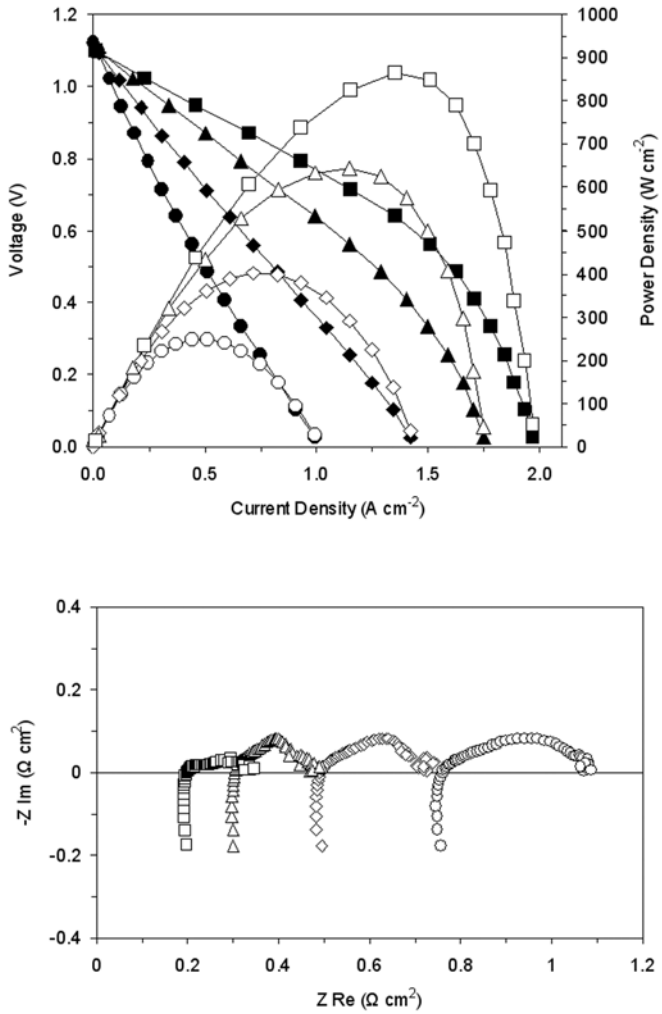

Figure 1 (a) V-i polarization curves and **(b)** impedance spectra on a 12 μm Ce-Pd-YSZ anode with a Ag current collector in humidified H_2 (3% H_2O). Data are shown for the following temperatures: circles, 923 K; diamonds, 973 K; triangles, 1023 K; and squares, 1073 K.

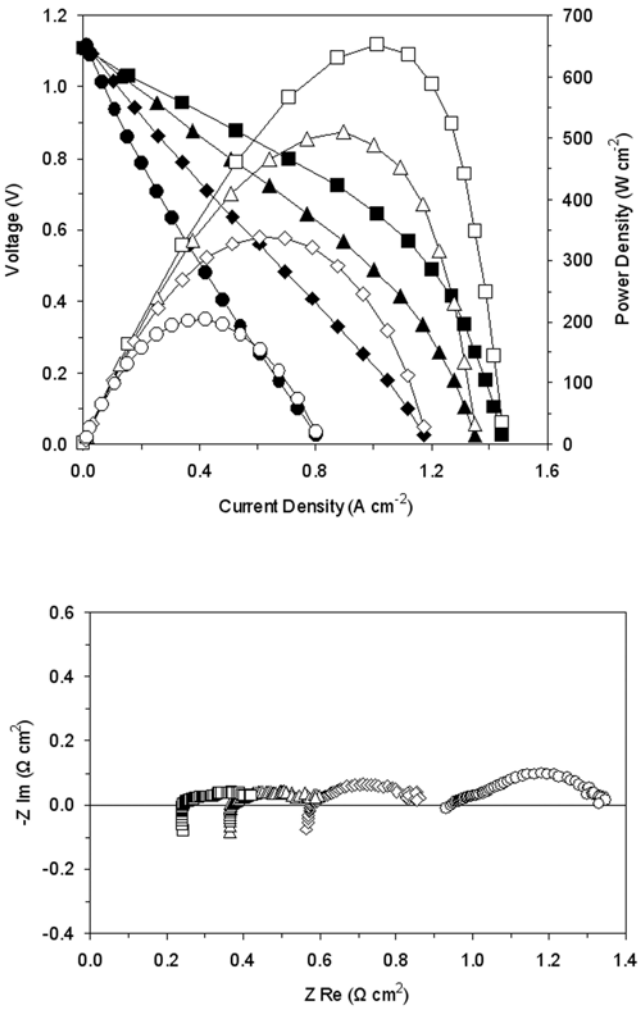

Figure 2 (a) V-i polarization curves and **(b)** impedance spectra on a 12 μm Ce-Pd-YSZ anode with a LST current collector in humidified H_2 (3% H_2O). Data are shown for the following temperatures: circles, 923 K; diamonds, 973 K; triangles, 1023 K; and squares, 1073 K.

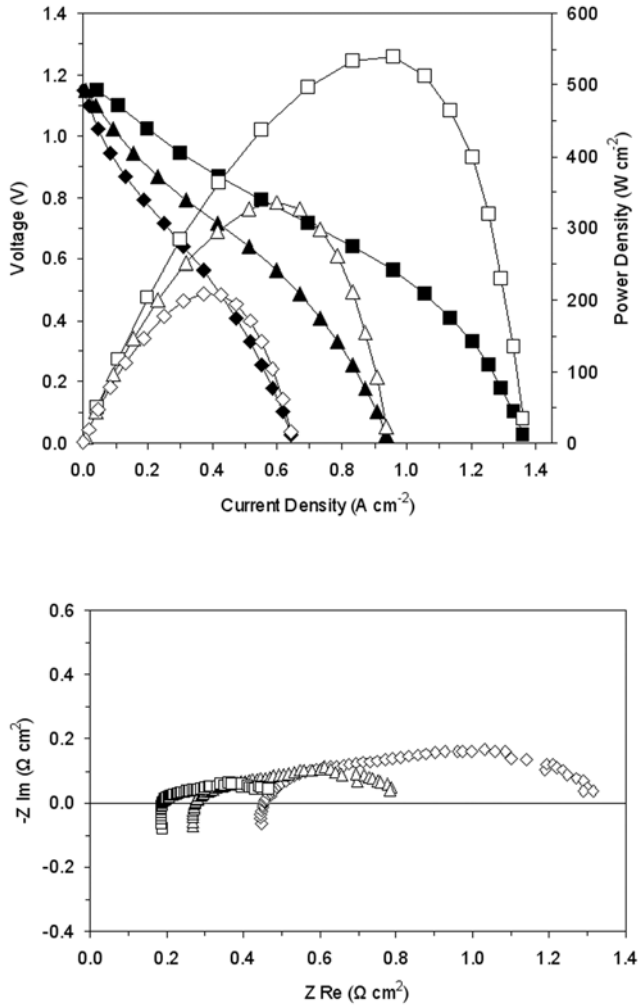

Figure 3 (a) V-i polarization curves and **(b)** impedance spectra on a 12 μm Ce-Pd-YSZ anode with a LST current collector in humidified CH_4 (3% H_2O). Data are shown for the following temperatures: diamonds, 973 K; triangles, 1023 K; and squares, 1073 K.

Table 1 Comparison of maximum power densities and ohmic resistances of cells with thin functional layer anodes.

sample	fuel*	923 K		973 K		1023 K		1073 K	
		P_{max} mW cm^{-2}	R_Ω Ω cm^2	P_{max} mW cm^{-2}	R_Ω Ω cm^2	P_{max} mW cm^{-2}	R_Ω Ω cm^2	P_{max} mW cm^{-2}	R_Ω Ω cm^2
12 μm Pd-Ce-YSZ	H_2	249	0.76	401	0.49	646	0.31	865	0.2
12 μm Ce-YSZ	H_2			88	0.55	144	0.38	261	0.27
50 μm Pd-Ce-YSZ	H_2	148	1.11	224	0.74	335	0.44	408	0.29
12 μm LST-Pd-Ce-YSZ	H_2	203	0.95	339	0.58	509	0.37	653	0.24
	CH_4			208	0.45	335	0.27	539	0.2

*fuels were humidified (3% H_2O)

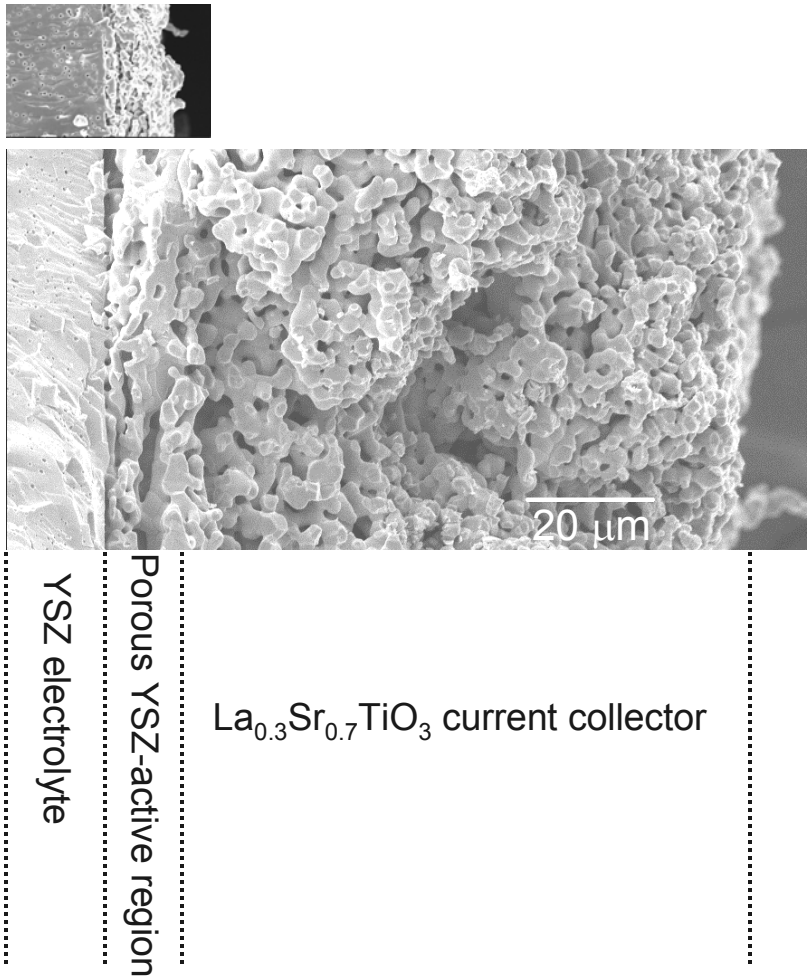

Figure 4 SEM micrographs of the anode region, prior to the addition of catalysts, of the cells used in this study.